

A STUDY ON THE ALUMINIZING OF ELECTRODEPOSITED NICKEL AT 500 °C

A.M. Rashidi^{1,2} and A. Amadeh^{1,*}

* amadeh@ut.ac.ir

Received: January 2010

Accepted: April 2010

¹ Department of Metallurgy and Materials Engineering, Faculty of Engineering, University of Tehran, Tehran, Iran.

² Faculty of Engineering, Razi University, Kermanshah, Iran.

Abstract: In this research, aluminizing behavior of ultra fine-grained nickel was investigated. For this purpose, nanocrystalline nickel samples with the grain size of ~25 nm were prepared via direct current electrodeposition and aluminized for different durations by pack cementation method at 500 °C. The aluminide layers were examined by means of SEM, EDS and XRD techniques. According to results, short time aluminizing resulted in the formation of a single aluminide layer whereas at long duration two distinct aluminide layers were formed. The growth kinetics of the coating was non-parabolic at short times while it obeyed the parabolic law at long duration. The parabolic growth rate constant of single phase coating formed on electrodeposited samples was about 30 $\mu\text{m}^2/\text{h}$ approximately 3 times greater than the data reported for coarse grained nickel (8.4 $\mu\text{m}^2/\text{h}$). Meanwhile, the overall growth rate constant was decreased to 11.7 $\mu\text{m}^2/\text{h}$, when double aluminide layers formed on nanocrystalline nickel.

Keywords: Aluminide; Coatings; Kinetics; Nanocrystalline; Nickel.

1. INTRODUCTION

The formation of diffusion coatings of nickel aluminides is of great interest in numerous technical applications ranging from metallization layers in microelectronics [1] to heat and corrosion resistant coatings applied on nickel-based superalloys [2,3]. There are diverse methods to apply aluminide coatings on superalloys [4-6], among them the so-called pack cementation is frequently used in practice [6,7]. This method was invented about 97 years ago by Van Aller [8] and several studies have been conducted dealing with its kinetics and mechanisms [9-16].

In pack cementation technique, the articles to be coated are embedded in a mixture of Al, an activator such as NH_4Cl , with or without Al_2O_3 powders, followed by heating at temperatures above 700 °C [16]. During heating process, the coating is formed via reduction reactions of metal halide vapors at the substrate surface and subsequent solid state diffusion of Al, and/or substrate species. When the supply of Al from the gaseous phase is freely available, the growth of the coating is controlled by solid-state diffusion and therefore the growth kinetics of formation of coating follows the 'parabolic growth kinetics' [13]:

$$y = k (t - t_0)^{1/2} \quad (1)$$

in which y is the thickness of the formed layer, k is the parabolic growth rate constant, t and t_0 are the aluminizing and delay times, respectively.

On the other hand, nowadays, the grain refinement of crystalline materials to nanometric size (less than 100 nm) is well known as the most beneficial way of improving their properties [17-20]. One of the important consequences of nanocrystallization of materials is extremely enhancement of reactive interfaces such as grain boundaries and triple junctions [18-20] and so, the diffusivity of elements in solids [21-23]. For example, the grain boundary self diffusivity of nanocrystalline nickel at the temperature range of 293- 423 K, is 21-34 orders of magnitude higher than the lattice self diffusivity in coarse grained nickel [24].

Based on the superior diffusivity of nanocrystalline materials, it seems that the refinement of grains to nanoscale size can be a helpful approach to improve diffusion-based processes such as gas nitriding and aluminizing. For example, the data reported [25] for gas nitriding of steel indicated that the thickness of nitride layer formed on nanocrystalline steel was approximately two times greater than coarse

grained samples. It was also demonstrated [26-28] that the heating time and temperature for formation of aluminide layers on steel considerably reduced using pack cementation assisted by ball-milling which was related to grain refinement down to nanoscale size. The aim of the present work is to examine the possibility of similar effect for unalloyed nickel. For this propose the formation and the growth kinetics of aluminide coating on electrodeposited nanocrystalline nickel has been investigated and compared to the results reported for aluminide coatings on coarse grained nickel.

2. EXPERIMENTAL PROCEDURE

Nanocrystalline nickel samples were prepared by direct current electroplating from the Watts type bath at the current density of 100 mA/cm². The details of the electrolyte composition as well as other deposition parameters have been described elsewhere [29]. After plating, the copper substrate was stripped away from the nickel layer by immersion of deposited samples in an aqueous chromic acid solution containing 250 g/l CrO₃ and 15 ml/l H₂SO₄ [30] at room temperature. The average grain size of electrodeposits was determined from X-ray diffraction peak broadening using modified Williamson–Hall equation [31-32]. An annealed nickel sample was used as the reference sample for correction of instrumental peak broadening

Prior to aluminizing treatment, the pack

cement consisted of 98 wt.% of Al powder as aluminum source and 2 wt.% of NH₄Cl as the activator was mechanically blended to obtain a homogenous mixture. It has been demonstrated [15] that the use of this mixture may lower the temperature of aluminizing of nickel and nickel alloys down to 500 °C. The samples were encased in the pack mixture placed in prealuminized cylindrical stainless steel retorts. The retorts were then sealed and subsequently heated in a resistance furnace to 500 °C for various durations in an argon atmosphere. After aluminizing, the cross section of coated specimens was studied by means of optical microscope and scanning electron microscope (SEM)² equipped with energy-dispersive X-ray spectrometer (EDS). The aluminide phases formed on the surface of the samples were identified by X-ray diffraction (XRD) using a Philips X'Pert-Pro instrument operated at 40 kV and 30 mA with CoK_α radiation ($\lambda=1.789\text{\AA}$) at a scan rate of 0.05 °s⁻¹ in the range of 40–130° and 0.02° step size.

3. RESULTS AND DISCUSSION

3.1. Morphology

The SEM micrographs of surface morphology of annealed and electrodeposited samples were presented in Fig.1a and Fig.1b, respectively. Large grains with the size in the micrometer range are observed in Fig.1a. As seen in Fig.1b, the electrodeposited nickel shows a colony-like

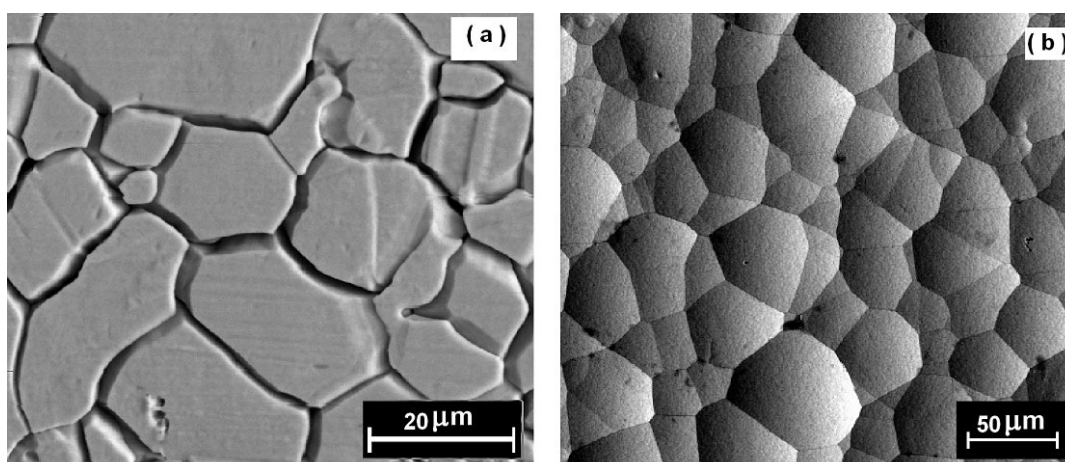


Fig. 1. SEM surface micrographs of a) annealed sample, and b) electrodeposited sample.

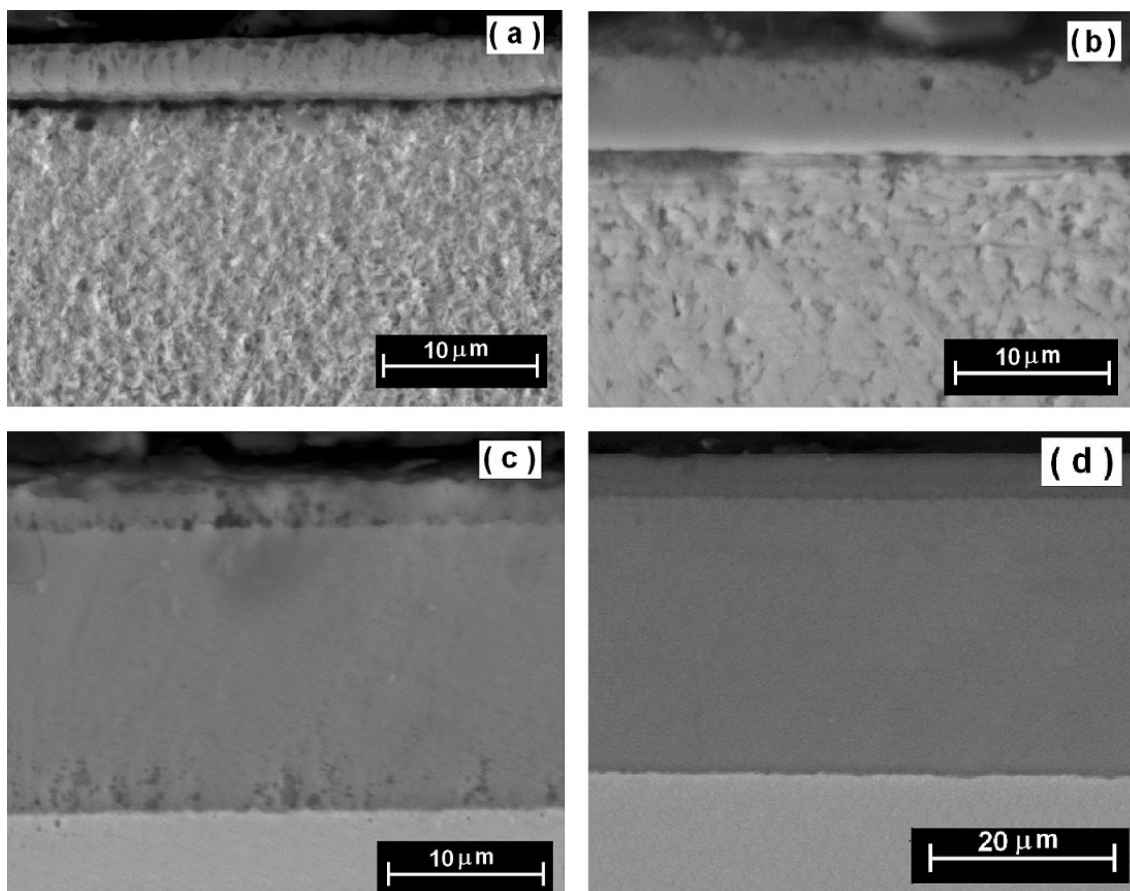


Fig. 2. SEM micrographs of the cross section of the samples aluminized for a) 1 h, b) 2 h, c) 4 h, and d) 8 h.

morphology consistent with the work of El-Sherik et al. [33] and Panek et al. [34]. Each colony is composed of several hundreds nano-sized grains, as shown by El-Sherik and Erb using transmission electron microscopy (TEM) [33].

The SEM micrographs of the cross section of nanocrystalline specimens aluminized for various durations were shown in Fig. 2. The coating formed on the samples aluminized for 1 h. and 2 h. is single layer as seen in Figs. 2a and 2b. In contrast, Figs. 3c and 3d indicates that the coating formed on samples aluminized for 4 h. and/or more, is composed of two layers.

3.2. Phase Analysis

The XRD patterns of annealed and electrodeposited samples were presented in Fig. 3. It can be observed that the crystal structure of the coatings is pure fcc nickel. The peak

broadening of electrodeposited coatings with respect to reference (annealed) sample is evident in this figure. According to line-broadening theory, the peak width difference between the reference sample and investigated specimens becomes readily observable when the grain sizes are in the nanometer ranges especially less than 50 nm [35]. The average grain size of electrodeposited sample calculated from XRD peak broadening using modified Williamson–Hall equation [30,31] was ~25 nm.

According to XRD patterns (Fig. 4a), the single layer coating is composed of Al_3Ni_2 phase. This finding is consistent with the work of Tamarin [15], who produced aluminide coating on coarse grained nickel at temperatures below 640 °C, using pack cementation and observed that the aluminide coating produced on pure nickel was single layer of Al_3Ni_2 phase. In contrast, XRD patterns of double layer coating (Fig.4b) indicates that the coating formed on the



Fig. 3. XRD patterns of annealed (reference) sample and electrodeposited nickel.

sample aluminized for 4 h and more consists of both Al_3Ni and Al_3Ni_2 phases. The composition of the outer and inner layers was also determined by EDS microanalysis. The aluminum content in outer layer was 58.7 wt.% near the composition of Al_3Ni phase. A concentration gradient was distinguished across the inner layer so that the concentration of Al at the adjacency of outer layer was 45.9 wt.% while it was 40.7 wt.% near the substrate. Considering the error of EDS technique, the measured values were consistent with the composition range of Al_3Ni_2 phase according to Al-Ni phase diagram. Therefore, according to EDS analysis and XRD patterns, the outer and inner aluminide layers formed on the specimens aluminized for 4 h. and/or more are Al_3Ni and Al_3Ni_2 phases, respectively.

In contrast to the absence of Al_3Ni phase on the surface of aluminized coarse grained nickel, its formation on nanocrystalline samples can be related to a barrier of phase formation. Whenever a new phase attempts to form, the energy required

to create a new interface will serve as a formation barrier [36]. The presence of high energy interfaces such as grain boundaries and triple junctions [18-20] and also grain-boundary dislocations [37] in nanocrystalline specimens provide the energy required overcoming the kinetic barriers and therefore, the formation of Al_3Ni phase on nanocrystalline nickel can occur.

3.3. Growth Kinetics

In general, the growth characteristics for a given layer are determined by plotting the thickness of the layer versus the square root of treating time ($t^{1/2}$). Hence, the thickness of aluminide coating as a function of the square root of aluminizing time was shown in Fig. 5. For comparison, the data reported by Tamarin [15] for coarse grained nickel was also presented. Normally, a linear plot is expected for such variation because during aluminizing treatment at low temperatures, the aluminide phase forms by



Fig. 4. XRD patterns of the samples aluminized for a) 2 h, and b) 4 h.

diffusion of aluminum into the substrate and/or intermetallic layers [15] and the kinetics of this process is expected to follow the parabolic growth law [13]. But in contrast to the data reported by Tamarin[15], three explicit regions can be distinguished in Fig. 5. Although in both regions II and III, the variation of the thickness of aluminide layer versus the square root of time is linear (with different slopes), in region I (early stages of aluminizing), there is a deviation from the parabolic growth law. A possible explanation for this deviation can be derived from the process controlled growth. In general, the growth kinetics of a single compound layer is determined by combination of two processes, namely (i) diffusion of the matter across the compound layer and (ii) rearrangement of the atoms at the interfaces required for the growth of the compound layer [38]. If the diffusion process is rate limiting, the layer thickness increases proportional to the square root of time, whereas if the interfacial reaction barriers control the kinetics, the increase in layer thickness with time is not parabolic. As described by Gosele and Tu [38], the growth kinetics is interface-controlled,

when the thickness of the layer is less than a changeover thickness, x^* , defined by:

$$x^* = D / k_{\text{eff}} \quad (2)$$

where D is interdiffusion coefficient and k_{eff} is effective interfacial reaction barrier.

As mentioned in the previous section, the grain refinement into nanometric size drastically increases the fraction of reactive and high energy interfaces which act as preferential sites for nucleation and, compared to coarse grained samples, open the additional reaction paths for fast nucleation of new phase at early reaction stages. Therefore, not only the formation of the first layer on nanocrystalline samples at early reaction stages can be faster, but also the formed phase would have a fine microstructure with relatively high density of active sites. Subsequently, the diffusivity of first layer formed on nanocrystalline specimens can be considerably higher than the diffusivity of the phases formed on coarse grained samples. This leads, according to equation 2, to a sufficiently large changeover thickness which implies a

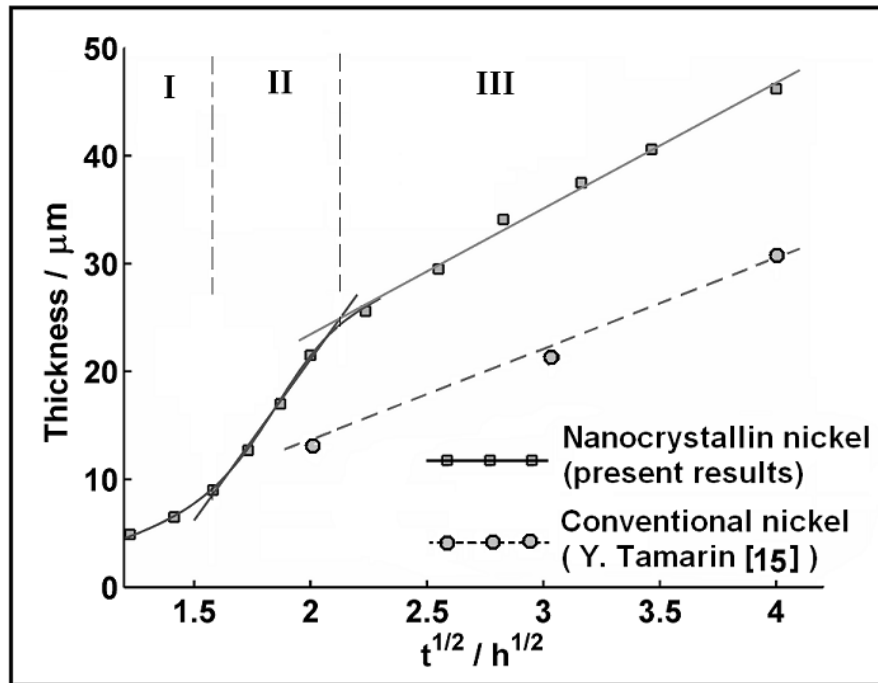


Fig. 5. The growth kinetics of aluminide coating formed on nanocrystalline nickel and coarse grained nickel [15].

relatively long duration of growth with interface-controlled kinetics. Consequently, at early stages of aluminizing of nanocrystalline nickel, the non-parabolic growth kinetics can be observed, as seen in region I in Fig. 5.

As the time proceeds and the coating grows to a thickness sufficiently larger than x^* , the interface-controlled growth kinetics will be substituted by diffusion-controlled growth kinetics. Therefore, after the initial transition period, it can be expected that the growth of aluminide coating on nanocrystalline nickel obeys the parabolic law. However, it can be observed in Fig. 5 that the growth rate constant of aluminide layers on nanocrystalline nickel is different from coarse grained one. In region II, the growth rate constant of nanocrystalline sample ($\sim 30 \mu\text{m}/h^{1/2}$) is approximately 3 times greater than coarse grained specimen ($8.4 \mu\text{m}/h^{1/2}$). Meanwhile, for aluminizing times higher than 4 h, the overall growth rate constant of the coating on nanocrystalline nickel decreases to $11.7 \mu\text{m}/h^{1/2}$ near to coarse grained nickel. Regarding to Fig. 2c, this reduction in growth rate constant after 4 h. of aluminizing could be attributed to the formation of a continuous Al_3Ni

layer. Based on the extrapolation of the data presented by Garcia et al. [39], the diffusion coefficient of Al in Al_3Ni and Al_3Ni_2 phases at 500°C is cm^2/s and cm^2/s , respectively. These values indicate that the growth of Al_3Ni layer is very slower than Al_3Ni_2 layer, as shown experimentally by Jung et al. [40]. Therefore, the growth of overall aluminide layers is controlled by the growth of Al_3Ni layer. Consequently, the overall growth rate constant decreases after the formation of Al_3Ni layer, as seen in Fig. 5.

4. CONCLUSIONS

The following conclusions can be made from the obtained results:

1. Aluminizing of nanocrystalline nickel led to formation of double Al_3Ni and Al_3Ni_2 layers beyond 4 h. of aluminizing time.
2. The growth kinetics of aluminide coating on nanocrystalline nickel did not obey the parabolic law at initial times of aluminizing.
3. Nanocrystallization of nickel accelerated the formation of aluminide coating in short aluminizing times with respect to coarse

grained nickel which was not the case at long times after the formation of Al_3Ni layer.

REFERENCES

1. Miracle, D.B., *The Physical and Mechanical Properties of NiAl*, *Acta Metall. Mater.*, 1993, 41, 649.
2. Svensson, H., Angenete, J. and Stiller, K., *Microstructure of Oxide Scales on Aluminide Diffusion Coatings After Short Time Oxidation at 1050 °C*, *Surf. Coat. Technol.*, 2004, 177-178, 152.
3. Rastegari, S., Arabi, H., Aboutalebi, M.R. and Eslami, A., *A Study on the Microstructural Changes of Cr-Modified Aluminide Coatings on a Nickel-Based Superalloy During Hot Corrosion*, *Can. J. Metall. Mater. Sci.*, 2008, 47, 223.
4. Goward, G.W. and Seigle, L.L., *Surface Engineering*, *ASM Handbook*, Vol. 5, *ASM International*, 1994, pp. 611-617
5. Chatterji, D., DeVries, R.C., and Romeo G., *Advances in Corrosion Science and Technology*, Vol. 6, eds. Fontana, M.G. and Staehle, R.W., Plenum Press, New York, USA, 1976, pp.1-87
6. Goward, G.W., *Progress in Coatings for Gas Turbine Airfoils*, *Surf. Coat. Technol.*, 1998, 108-109, 73.
7. Thevand, A. Poizet, S., Crousier, J.P. and Streiff, R., *Aluminization of Nickel- Formation of Intermetallic Phases and Ni₂Al₃ Coatings*, *J. Mater. Sci.*, 1981, 16, 2467.
8. Van Aller, T., Treatment of metals, US Patent 1155974, 1911.
9. Gupta, B.K. Sarkhel, A.K. and Seigle, L.L., *On the Kinetics of Pack Aluminization*, *Thin Solid Films*, 1976, 39, 313.
10. Gupta, B.K. and Seigle, L.L., *The Effect On the Kinetics of Pack Aluminization of Varying the Activator*, *Thin Solid Films*, 1980, 73, 365.
11. Sivakumar, R. and Seigle, L.L., *On the Kinetics of the Pack-Aluminization Process*, *Metall. Trans.*, 1976, 7A, 1073.
12. Arabi, H., Rastegari, S. and Sadeghi, B. M., *Effect of Aluminizing Parameters On the Microstructure and Thickness of Pt-Aluminide Coating Applied on a Ni-Base Superalloy GTD111*, *Iranian J. Mater. Sci. Eng.*, 2004, 1, 65.
13. Hick, A.J. and Heckel, R.W., *Kinetics of Phase Layer Growth During Aluminide Coating On Nickel*, *Metall. Trans.*, 1975, 6A, 431.
14. Goward, G.W. and Boone, D.H., *Formation and Degradation Mechanisms of Aluminide Coatings On Nickel Base Superalloys*, *Oxid. Met.*, 1971, 3, 475.
15. Tamarin, Y., *Protective Coatings for Turbine Blades*, Ohio, Materials Park, ASM Inter., 2002. PP. 25-78
16. Xiang, Z.D., Burnell-Gray, J.S. and Datta, P.K., *Aluminide Coating Formation On Nickel-Base Superalloys by Pack Cementation Process*, *J. Mater. Sci.*, 2001, 36, 5673.
17. Torabi, M., Khalifehzadeh, R., Arami, H. and Sadrnezhad, S.K., *Electrochemical Deposition of Flower-like Nickel Nanostructures On Well-defined n-Si(111):H*, *IJE.*, 2008, 21B, 177.
18. Tjong, S.C. and Chen, H., *Nanocrystalline Materials and Coatings*, *Mater. Sci. Eng.*, 2004, 45 R, 1.
19. Murty, B.S., Data, M.K. and Pabi, S.K., *Structure and Thermal Stability of Nanocrystalline Materials*, *Sadhana*, 2003, 28, 23.
20. Gleiter, H., *Nanostructured Materials: Basic Concepts and Microstructure*, *Acta Mater.*, 2000, 48, 1.
21. Belova, I.V. and Murch, G.E., *Diffusion in Nanocrystalline Materials*, *J. Phys. Chem. Solids*, 2003, 64, 873.
22. Chattopadhyay, P.P., Pabi, S.K. and Manna, I., *On the Enhancement of Diffusion Kinetics in Nanocrystalline Materials*, *Mater. Chem. Phys.*, 2001, 68, 80.
23. Wurschum, R., Herth, S. and Brossann, U., *Diffusion in Nanocrystalline Metals and Alloys - A Status Report*, *Adv. Eng. Mater.*, 2005, 5, 365.
24. Bokstein, B.S., Bröse, H.D., Trusov, L.I. and Khvostantseva, T.P., *Diffusion in Nanocrystalline Nickel*, *Nanostr. Mater.*, 1995, 6, 873.
25. Gu, J.F., Bei, D.H., Pan, J.S., Lu, J. and Lu, K., *Improved Nitrogen Transport in Surface Nanocrystallized Low-Carbon Steels During*

- Gaseous Nitridation, *Mater. Lett.*, 2002, 55, 340.
26. Zhan, Z., He, Y., Wang, D. and Gao, W., Low-Temperature Processing of Fe–Al Intermetallic Coatings Assisted by Ball Milling, *Intermetallics*, 2006, 14, 75.
27. Zhan, Z., He, Y., Wang, D. and Gao, W., Aluminide Coatings Formed On Fe–13Cr Steel at Low Temperature and Its Oxidation Resistance, *Oxid. Met.*, 2007, 68, 243.
28. Zhan, Z., He, Y., Wang, D. and Gao, W., Preparation of Aluminide Coatings at Relatively Low Temperatures, *Trans. Nonferrous Met. Soc. China*, 2006, 16, 647.
29. Rashidi, A.M. and Amadeh, A., The Effect of Current Density On the Grain Size of Electrodeposited Nanocrystalline Nickel Coatings, *Surf. Coat. Technol.*, 2008, 202, 3772.
30. Giga, A., Kimoto, Y., Takigawa, Y. and Higashi, K. Demonstration of an Inverse Hall–Petch Relationship in Electrodeposited Nanocrystalline Ni–W Alloys Through Tensile Testing, *Scr. Mater.*, 2006, 55, 143.
31. Ungár, T., Gubicza, J., Ribárik, G. and Borbély, A., Crystallite Size Distribution and Dislocation Structure Determined by Diffraction Profile Analysis: Principles and Practical Application to Cubic and Hexagonal Crystals, *J. Appl. Cryst.*, 2001, 34, 298.
32. Ungár, T., Characterization of Nanocrystalline Materials by X-ray Line Profile Analysis, *J. Mater. Sci.*, 2007, 42, 1584.
33. El-Sherik, A.M. and Erb, U., Synthesis of Bulk Nanocrystalline Nickel by Pulsed Electrodeposition, *J. Mater. Sci.*, 1995, 30, 5743.
34. Panek, J., Budniok, A. and Lagiewka, E., Electrochemical Production and Characterization of Ni-Based Composite Coatings Containing Mo Particles, *Rev. Adv. Mater. Sci.*, 2007, 15, 234.
35. Waren, B.E., X-Ray Diffraction Methods, *J. Appl. Phys.*, 1941, 12, 375.
36. Schmelzer, J.W.P., Kinetic and Thermodynamic Theories of Nucleation, *Mater. Phys. Mech.*, 2003, 6, 21.
37. Ovid'ko, I.A. and Sheinerman, A.G., Diffusion Percolation Along Triple Junctions in Nanocrystalline Materials, *Rev. Adv. Mater. Sci.*, 2004, 6, 41.
38. Gosele, U. and Tu, K.N., Growth Kinetics of Planar Binary Diffusion Couples: Thin-Film Case Versus Bulk Cases, *J. Appl. Phys.*, 1982, 53, 3252.
39. Garcia, V.H., Mors, P.M. and Scherrer, C., Kinetics of Phase Formation in Binary Thin Films: the Ni/Al Case, *Acta Mater.*, 2000, 48, 1201.
40. Jung, S.B., Minamino, Y., Yamane, T. and Saji, S., Reaction Diffusion and Formation of Al₃Ni and Al₃Ni₂ Phases in the Al–Ni System, *J. Mater. Sci. Lett.*, 1993, 12, 1684.